

UC Davis

UC Davis Previously Published Works

Title

Cell-secreted extracellular matrix, independent of cell source, promotes the osteogenic differentiation of human stromal vascular fraction

Permalink

<https://escholarship.org/uc/item/8zq631x4>

Journal

Journal of Materials Chemistry B, 6(24)

ISSN

2050-750X

Authors

Harvestine, Jenna N
Orbay, Hakan
Chen, Jonathan Y
[et al.](#)

Publication Date

2018-06-28

DOI

10.1039/c7tb02787g

Peer reviewed



Published in final edited form as:

J Mater Chem B. 2018 June 28; 6(24): 4104–4115. doi:10.1039/C7TB02787G.

Cell-secreted extracellular matrix, independent of cell source, promotes the osteogenic differentiation of human stromal vascular fraction

Jenna N. Harvestine, B.S.^a, Hakan Orbay, M.D., Ph.D.^b, Jonathan Y. Chen^a, David E. Sahar, M.D.^b, and J. Kent Leach, Ph.D.^{a,c,*}

^aDepartment of Biomedical Engineering, University of California, Davis, Davis, CA 95616

^bDepartment of Surgery, Division of Plastic Surgery, UC Davis Health, Sacramento, CA 95817

^cDepartment of Orthopaedic Surgery, School of Medicine, UC Davis Health, Sacramento, CA 95817

Abstract

Lipoaspirates contain a readily accessible heterogeneous cell source for use in bone regeneration collectively referred to as the stromal vascular fraction (SVF). However, the osteogenic potential of SVF is inferior to other progenitor cell populations, thereby requiring alternative strategies to potentiate its effective use in cell-based therapies of bone repair. Cell-secreted extracellular matrix (ECM) is a promising substrate to guide cell phenotype or for use in biomaterial design, yet the instructional capacity of ECMs produced by various cell types is unknown. To determine whether the bioactivity of cell-secreted ECM was dependent on cell source, we assessed the osteogenic response of human SVF on ECMs secreted by bone marrow-derived mesenchymal stem cells (MSCs), adipose stromal cells (ASCs), and human dermal fibroblasts (HDFs). Tissue culture plastic (TCP), type I collagen, and ECM induced expression of integrin subunits α_2 , α_5 , and β_1 in SVF, yet seeding efficiency was only improved on MSC-derived ECM. Regardless of ECM source, SVF deposited over 8- and 1.3-fold more calcium compared to TCP and collagen-coated controls, respectively. Flow cytometry confirmed that SVF cultured on ECM retained CD31 and CD34 positive cell populations better than TCP. After depleting accessory cells, ASCs deposited significantly less calcium compared to donor-matched SVF. This function was partially restored in the presence of MSC-derived ECM when donor-matched endothelial cells (ECs) were added in an

*Address for correspondence: J. Kent Leach, Ph.D., University of California, Davis, Department of Biomedical Engineering, 451 Health Sciences Drive, Davis, CA 95616, jkleach@ucdavis.edu.

Author Information

Jenna N. Harvestine, B.S., University of California, Davis, Department of Biomedical Engineering, 451 Health Sciences Drive, Davis, CA 95616, jnharvestine@ucdavis.edu

Hakan Orbay, M.D., Ph.D., Department of Surgery, Division of Plastic Surgery, UC Davis Health, Research II Building, 4625 2nd Avenue, Sacramento, CA 95817, hakanorbay78@gmail.com

Jonathan Y. Chen, University of California, Davis, Department of Biomedical Engineering, 451 Health Sciences Drive, Davis, CA 95616, jthchen@ucdavis.edu

David E. Sahar, M.D., Department of Surgery, Division of Plastic Surgery, UC Davis Health, 2221 Stockton Boulevard, Suite 2123, Sacramento, CA 95817, desahar@ucdavis.edu

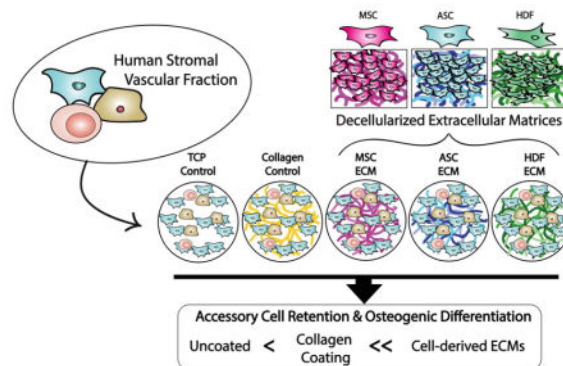
Reprint Author: J. Kent Leach, Ph.D., University of California, Davis, Department of Biomedical Engineering, 451 Health Sciences Drive, Davis, CA 95616, jkleach@ucdavis.edu

CONFLICTS OF INTEREST

No competing financial interests exist.

ASC/EC co-culture, confirming a role for ECs in osteogenic differentiation. These findings support the use of cell-derived ECM as a means to promote cell retention and osteogenic differentiation of SVF.

Graphical Abstract



Keywords

extracellular matrix; osteogenesis; stromal vascular fraction; co-culture; accessory cells

1. INTRODUCTION

The extracellular matrix (ECM) is the fabric that supports tissue-specific functions of associated cells by presenting a complex milieu of soluble and insoluble signals.¹ Essential ECM components have been identified that promote cell adhesion, migration, self-assembly into larger structures, and differentiation.^{2, 3} However, this bottom-up approach to biomaterials design, commonly employing individual proteins or functional peptide sequences of proteins, fails to capture beneficial interactions with other ligands and restricts the potential benefit of ECMs to guide cell fate.

Cell-secreted ECMs preserve the complex nature of ECMs and have utility as bioactive platforms to instruct stem and progenitor cells.⁴ Following decellularization, acellular ECMs can be used as coatings on various substrates to recapitulate physical and chemical cues that guide cell function.⁵⁻⁸ For example, we demonstrated the efficacy of a bone marrow-derived mesenchymal stem cell (MSC)-secreted ECM to promote MSC trophic factor secretion, survival, osteogenic differentiation, and bone formation *in vivo*.⁹⁻¹³ The limited number of MSCs within bone marrow aspirations and lasting patient discomfort following collection represent significant challenges to harvesting MSCs for producing ECM as a biomaterial. Moreover, Ragelle *et al.* reported stem cell-specific proteomic composition and cell response to cell-derived ECMs.¹⁴ Therefore, the potential of other readily accessible cell populations to secrete an osteoinductive matrix warrants further investigation. To address this knowledge gap, this work compares the osteoinductive capacity of MSC-derived ECM to matrices produced using more readily accessible cell types, including human adipose-derived stromal cells (ASCs) and human dermal fibroblasts (HDFs).

A reliable and economical source of autologous progenitor cells is an integral component to propel tissue engineered therapies into the clinical setting. Bone marrow aspirates do not supply a sufficient number of cells, requiring *ex vivo* cell expansion to reach the desired cell density for re-implantation. The culture expansion of cells under Good Manufacturing Practice standards can be costly and limit clinical translation, further motivating the investigation into alternative cell sources that may be used with minimal manipulation. Adipose stromal cells (ASCs) can be isolated in greater numbers from adipose tissue obtained *via* liposuction, a less invasive procedure than bone marrow aspiration. The volume of cells obtained from lipoaspirate, collectively referred to as the stromal vascular fraction (SVF), contains stromal, endothelial, and hematopoietic cells.¹⁵ Compared to bone marrow aspirates, stromal cells can be isolated at 10–100 fold higher frequency from SVF.¹⁶ However, ASCs exhibit comparable or reduced osteogenic potential,¹⁷ motivating the need for improved methods to enhance osteogenic potential of SVF.

We hypothesized that the bioactivity of cell-secreted ECM is dependent upon the identity of the secreting cell. To investigate this hypothesis, we assessed the osteogenic response of SVF on ECMs produced by human MSCs, ASCs, and dermal fibroblasts (HDFs), three common cell populations used to manufacture ECM due to their accessibility and proliferative potential. We compared the composition, osteogenic potential, and capacity to retain SVF cells from primary adipose tissue for each ECM. The results of this study support the use of cell-secreted ECMs to enhance the therapeutic potential of SVF.

2. MATERIALS AND METHODS

2.1 Cell culture

Human bone marrow-derived MSCs, ASCs, and HDFs (Lonza, Walkersville, MD) were used without further characterization. MSCs were expanded under standard conditions until use at passages 4–6 in minimum essential alpha medium (α -MEM; w/L-glutamine, w/o ribo/deoxyribonucleosides (Invitrogen, Carlsbad, CA)) supplemented with 10% fetal bovine serum (FBS; Atlanta Biologicals, Flowery Branch, GA) and 1% penicillin (10,000 U mL⁻¹) and streptomycin (10 mg mL⁻¹, Mediatech, Manassas, VA) (P/S). ASCs were expanded under standard conditions until use at passages 4–6 in Dulbecco's modified eagle medium (DMEM; Invitrogen) supplemented with 10% FBS and 1% P/S. HDFs were expanded until use at passages 9–11 in low glucose DMEM (Invitrogen) supplemented with 10% FBS and 1% P/S.

2.2 ECM production and characterization

Cell-secreted ECMs were prepared as we described.^{9–13} Briefly MSCs, ASCs, or HDFs were seeded at 50,000 cell cm⁻² and cultured in media supplemented with 50 μ g mL⁻¹ ascorbate 2-phosphate for 10 days with media changes every 2–3 days. After culture, monolayers were washed with phosphate buffered saline (PBS) and cells were removed using a detergent-based solution followed by DNase (Sigma, St. Louis, MO) treatment (37°C for 1 hr) to effectively remove 99.9% of DNA content from culture post-decellularization.¹⁰ ECM morphology before and after decellularization was visualized using a Nikon Eclipse TE2000U microscope (Melville, NY, USA) and Andor Zyla digital

camera (Oxford Instruments, Abingdon, UK). Decellularized ECM was washed 3x with PBS and mechanically dislodged from culture flasks using a cell scraper. Total protein within the collected ECM was quantified using a bicinchoninic acid (BCA) protein assay (Thermo Fisher, Rockford, IL). ECM solutions were frozen at -20°C until use.

To prepare protein-coated substrates, ECM solutions were thawed and sonicated to generate a homogeneous distribution. Equal quantities of ECM or type I collagen (Fisher Scientific, Santa Clara, CA) were deposited on well plates ($15\ \mu\text{g cm}^{-2}$ unless otherwise stated) and spread using a micropipette. ECM and collagen solvents were allowed to evaporate, then wells were washed 2x with PBS prior to use. For gross visual inspection of ECM distribution, wells were washed with PBS, submerged for 15 min in 1% (w/v) Coomassie Brilliant Blue (MP Biomedicals, Solon, OH), and washed in PBS before imaging.¹² To measure glycosaminoglycan (GAG) content, ECMs were digested in papainase buffer at 60°C for 16 hrs and GAG was quantified using a dimethylmethylene blue (DMMB) assay.¹⁸ ECM composition was determined using liquid chromatography–mass spectrometry (LC-MS) by MS Bioworks, LLC (Ann Arbor, MI).¹⁹

2.3 Isolation of stromal vascular fraction (SVF)

Human SVF was harvested from adipose tissue samples retrieved *via* liposuction or excision from the abdomen, breast, and thigh of female patients ($n=10$; 40–75 years old, mean age 54 ± 10 years) after obtaining consent under an IRB protocol approved by UC Davis. Adipose tissue was cleaned and transferred to a new culture dish to be minced into small pieces as needed.²⁰ Minced tissue/lipoaspirate was digested in 0.1% (w/v) type I collagenase (Calbiochem, San Diego, CA) and 0.3 U dispase (Thermo Fisher) for 1 hr at 37°C with external agitation. Enzymes were quenched by the addition of an equal volume of growth medium containing FBS, and cells were pelleted by centrifugation at $1,000\times g$. Cells were incubated in a red blood cell lysis buffer (154.4 mM ammonium chloride, 10 mM potassium bicarbonate, and 97.3 mM EDTA tetrasodium salt)²¹ for 5 min at 37°C , washed with PBS, and resuspended in culture medium.

2.4 Characterization of SVF response to ECM coating

Directly after isolation, viable cells were quantified using a Countess® II Automated Cell Counter (Thermo Fisher) and plated onto TCP, type I collagen- or ECM-coated culture dishes at $30,000\ \text{cells cm}^{-2}$ in growth media composed of α -MEM supplemented with 10% FBS and 1% P/S. Media was refreshed after 24 hrs with osteogenic media composed of α -MEM supplemented with 10% FBS, 1% P/S, $50\ \mu\text{g mL}^{-1}$ ascorbate 2-phosphate, 10 mM β -glycerophosphate, and 10 nM dexamethasone (all from Sigma) and then every 3 days until collection. Cell metabolic activity was determined using an alamarBlue assay (Invitrogen) per the manufacturer's instructions. Prior to collection, cells were incubated in $2\ \mu\text{M}$ calcein AM (Invitrogen) at 37°C for 30 min, washed with PBS, and imaged to visualize viable cell morphology. Cell area was quantified from fluorescent images. Cell boundaries were traced, and total cell area was calculated in NIS Elements (Nikon Instruments Inc., Melville, NY).

To determine seeding efficiency and substrate-mediated integrin expression during adhesion, freshly isolated SVF was seeded on TCP, type I collagen-, or ECM-coated culture dishes in

growth media and collected after 7 hrs. Baseline DNA content and gene expression were determined from equal aliquots of cells in suspension. To interrogate integrin expression, samples were collected in TRIzol Reagent (Invitrogen) for PCR analysis following manufacturer's instructions. After RNA isolation, 600 ng of RNA was reverse transcribed with the QuantiTect Reverse Transcription kit (Qiagen, Valencia, CA) and qPCR was performed using Quantifast Probe PCR kit (Qiagen) on a QuantStudio5 system (Applied Biosystems). Primers and probes for housekeeping gene *RPL13* (Hs00744303_s1) and integrin subunits *ITGA1* (α_1 , HS01061271_M1), *ITGA2* (α_2 , HS00158127_M1), *ITGA5* (α_5 , HS01547673_M1), *ITGA10* (α_{10} , HS01006910_M1), and *ITGB1* (β_1 , HS01127536_M1) were purchased from Thermo Fisher. Amplification conditions were 95°C for 3 min, followed by 45 cycles at 95°C for 3 s and 60°C for 30 s. Quantitative PCR results were normalized to *RPL13* transcript levels to yield $-Ct$, and fold change in expression relative to the housekeeping gene was calculated using 2^{-Ct} .²² To evaluate seeding efficiency, samples were collected in passive lysis buffer (PLB, Promega, Sunnyvale, CA). Following a freeze-thaw cycle, the lysate was sonicated (10 s on ice) and centrifuged to pellet cell debris. DNA content of adherent cells was compared to viable cells from an aliquot of cell suspension using a Quant-iT PicoGreen dsDNA Assay Kit (Invitrogen).

2.5 Osteogenic differentiation of SVF and retention of endothelial cells on ECM

Cells were plated onto TCP, collagen-, or ECM-coated culture dishes at 30,000 cells cm^{-2} in growth media. After 24 hrs, media was refreshed with osteogenic media, and media was exchanged every 3 days. To collect samples, wells were rinsed in PBS, incubated in PLB and then in 0.9N H_2SO_4 and scraped for collection. DNA content was measured using a Quant-iT PicoGreen dsDNA Assay Kit (Invitrogen). Alkaline phosphatase (ALP) activity was quantified from cell lysate as described.²³ Calcium deposition was quantified using an α -cresolphthalein assay and visualized using a 2% Alizarin Red S solution (Sigma).¹⁰ Matrix composition and morphology was evaluated using a Masson's Trichrome staining kit (AB150686, Abcam, Cambridge, MA).

The identity of cells present after differentiation was determined by flow cytometry. Briefly, cells were immersed in trypsin under external agitation for 5 min at 37°C, followed by gentle scraping to detach cells from the culture dishes. Cell solutions were passed through a 41 μm filter (EMD Millipore) to remove ECM and washed in PBS. Non-specific binding was blocked by incubation in Protein Block (AB156024, Abcam, Cambridge, MA) for 30 min and then incubated with antibodies per manufacturer's instructions for CD31 (303110), CD45 (368518), CD34 (343623), CD90 (328112), and CD73 (344008) (all from BioLegend, San Diego, CA).

Donor-matched endothelial (CD31+) or adipose-derived stromal cells (CD271+) were selected from freshly isolated SVF by magnetic activated cell sorting (MACS). Briefly, freshly isolated, unfractionated SVF was incubated in microbead kits to select for endothelial (CD31 Microbead Kit, 130-091-935; Miltenyi Biotec, Auburn, CA) or stromal cells (CD271 Microbead Kit, 130-099-023; Miltenyi Biotec) following manufacturer's instructions. Positive selection of desired cell types was performed using MS columns in a

MidiMACS separator (Miltenyi Biotech). CD31+ cells were expanded under standard conditions until use at passage 2 in EGM-2 MV (PromoCell, Heidelberg, Germany). CD271+ cells were expanded under standard conditions until use at passage 2 in DMEM (Invitrogen) supplemented with 10% FBS and 1% P/S. To evaluate the contribution of endothelial cells to osteogenic differentiation, a co-culture containing 3:2 ratio of ASC:EC was seeded at 30,000 cells cm⁻² onto TCP, collagen-, or ECM-coated wells in GM. Donor-matched unfractionated SVF and monocultures of ECs or ASCs containing the same total cell number were used as controls. Media was changed to osteogenic media 24 hrs after plating, with media changes every 3 days until collection.

2.6 Statistical analysis

Data are presented as means \pm standard deviation of n=3–6 replicates from 2–3 biological donors unless otherwise stated. Statistical analyses were performed with two-way ANOVA, followed by Tukey's multiple comparison *post hoc* test (GraphPad Prism 7.0, San Diego, CA) to determine significance ($p < 0.05$). Significance is denoted by alphabetical letterings; groups with no significance are linked by the same letters, while groups with significance do not share a letter. A lack of significance between groups is indicated with "ns" and a line bridging non-significant groups.

3. RESULTS AND DISCUSSION

3.1 ECM composition and quantity are cell-type specific

Tissue decellularization is useful to generate biomaterials that retain the structure and composition of native tissues.²⁴ Matrices have been derived from numerous tissues including skeletal and cardiac muscle, cartilage, adipose, and others.^{25–28} Compelling evidence demonstrates that tissue-specific ECMs more effectively guide the function of cells that reside in that tissue.²⁹ The harvest of cell-secreted ECM from human cells in culture provides an alternative to whole tissue decellularization and an opportunity to tailor the ECM properties through manipulation of culture conditions.¹⁰ In this study, MSCs, ASCs, and HDFs each secreted ECM over a ten day protocol optimized for the production of an osteoinductive ECM.¹⁰ Following the culture, ECM was retrieved following a gentle detergent-based decellularization method. We selected these three cell populations for manufacturing ECM due to their relative ease of accessibility from donor patients, proliferative capacity for potential use in cell banking, and previous use.^{9–13, 30, 31} During ECM deposition, all cells exhibited characteristic spindle-like morphologies (Fig. 1A–C) and maintained a confluent sheet throughout culture. MSCs and HDFs were well-organized, demonstrating a compact cell arrangement, while ASCs were noticeably less organized and densely packed. After decellularization, the cell-secreted ECM could be visually observed with no discernable differences in gross morphology (Fig. 1D–F). All ECMs were briefly sonicated to mechanically homogenize the proteins into a spreadable solution and stained with Coomassie Brilliant Blue to view ECM protein distribution on tissue culture plates (Fig. 1G–I). Compared to ASC- and HDF-derived ECMs, MSC-derived ECMs exhibited a more homogeneous size distribution and ECM coverage on the culture surface.

To produce cell-derived ECM, equal numbers of MSCs, ASCs, or HDFs (50,000 cells cm⁻²) were seeded and cultured for 10 days prior to decellularization. Total protein content within secreted ECMs was measured after decellularization (Fig. 2A). MSC-derived ECM contained 15.1 ± 4.1 μg protein cm⁻², nearly 3-fold and 1.5-fold greater than the protein mass secreted by ASCs and HDFs, respectively. Considering the capacity to achieve greater numbers of ASCs and HDFs at the time of tissue harvest or due to their rapid proliferative potential, this may represent only a modest benefit for MSCs in producing cell-secreted ECMs. However, bone marrow aspiration only necessitates local anesthetic. In contrast, ASC collection often requires general anesthesia, and skin biopsy to retrieve autologous dermal fibroblasts results in a visible wound with the potential to scar. While ASCs and HDFs offer increased availability of accessible tissue, the impact of depot-specific characteristics and variability necessitate further investigation prior to widespread use.

Mass spectrometry analysis identified 278, 225, and 150 distinct proteins within MSC-, ASC-, and HDF-derived ECMs, respectively, suggesting that stromal cell-derived ECMs are more complex than HDF-derived ECMs which contained nearly 50% fewer distinct proteins. On average, collagens make up approximately 24% of total protein within MSC-derived ECMs, while ASC- and HDF-derived ECMs contain 36% and 53% collagen by mass, respectively (Fig. 2B). In agreement with other reports,⁵ when normalized to molecular weight, collagens represented the largest family of molecules in each ECM, representing 11.3%, 16.0%, and 24.3% of MSC-, ASC-, and HDF-derived ECM proteins, respectively. Type I collagen comprised 39%, 50%, and 69% of MSC-, ASC- and HDF-derived ECM total collagens (Fig. 2D). In contrast, others reported significantly higher levels of collagen VI and XII (85–90%) versus collagen I (10–15%) in ECM produced by bone marrow and adipose stromal cells that were used at lower passages and lower cell seeding densities.⁵ In this work, collagens III and V, which commonly associate with types I and VI, were well-represented in all ECMs. The number and type of remaining collagens present was ECM-specific. Interestingly, type IV collagen, a basement membrane protein important for blood vessel integrity, and type VIII collagen, found in the subendothelium and responsible for endothelial cell differentiation and angiogenesis, constituted 5.7% and 11%, respectively, of collagens within MSC-derived ECM. In contrast, type IV collagen represented 0.37% and 0.22% of ASC- and HDF-derived ECMs, and type VIII represented 1.2% of ASC-derived ECM yet was not present in HDF-derived ECM. Fibronectin, an ECM protein required for osteoblast mineralization,³² was a major component of MSC- and ASC-derived ECM. Conversely, HDF-derived ECM was dominated by collagens, containing less fibronectin than either stromal cell-derived ECM. Glycosaminoglycan (GAG) content within ECMs was minimal (less than 5% of ECM content). However, the greatest GAG content was observed in ASC-derived ECM compared to MSC- or HDF-derived EMCs (Fig. 2C). Various proteins associated with osteogenic differentiation, pro-angiogenic potential, and immunomodulation were identified within the ECMs (Table 1). Although each of these proteins are within the top 50 most abundant ECM proteins detected, the relative percentages are low due to the complexity and number of total proteins present.

3.2 ECM-coated wells support SVF adhesion, proliferation, and metabolic activity

We measured DNA content 7 hours after seeding to assess the contribution of ECM coatings to cell adhesion. While all substrates exhibited lower DNA content than the initial number of plated cells, SVF cultured on collagen-coated wells had significantly less DNA content compared to all other substrates (Fig. 3A). SVF seeded on MSC-derived ECMs achieved 73% seeding efficiency, significantly greater than all other substrates (Fig. 3B). In contrast, SVF on TCP and collagen exhibited 62% and 44% seeding efficiency, respectively.

To investigate if differences in seeding efficiency were due to substrate-specific integrin expression, we performed qPCR on freshly isolated cells and cells cultured for 7 hours. Freshly isolated cells had relatively low expression of integrin subunits α_1 , α_2 , α_5 , α_{10} , and β_1 (Fig. 3C). However, after 7 hours in culture, we detected strong expression of integrin subunits α_2 , α_5 , α_{10} and β_1 on all substrates. The β_1 integrin subunit binds various collagens, and the $\alpha_2\beta_1$ integrin pair binds fibrillar collagen. We previously demonstrated the critical role of $\alpha_2\beta_1$ on MSC adhesion to cell-secreted ECMs and retention of osteoblastic phenotype.^{11, 33} Integrin subunit α_2 was most highly expressed on collagen and ASC-derived ECM and exhibited the lowest expression on MSC-derived ECM (Fig. 3E). Similarly, expression of the α_5 subunit was greatest on ASC-derived ECM and least on MSC-derived ECM (Fig. 3F). Unlike other ECMs, MSC-derived ECM contained appreciable levels of collagens IV and VIII, both important for blood vessel formation and maintenance. Indeed, we observed increased expression of collagen IV-binding integrin subunit, α_{10} , on MSC-derived ECM (Fig. 3G). Expression of integrin subunits α_1 (Fig. 3D) and β_1 (Fig. 3H) were similar across all substrates.

The early benefits of seeding efficiency on MSC-derived ECMs were lost over time in culture, with cells proliferating consistently on all ECM substrates (Fig. 4A). During the first days of culture, cells remained rounded with relatively low metabolic activity (Fig. 4B–C). After 4 days in culture, there were appreciable increases in metabolic activity and elongation. In fact, cells were sub-confluent and distinct cell morphologies were clearly visible, suggesting that substrates may differentially retain various cell types from the heterogeneous SVF population. Quantification of cell area revealed substrate-specific morphologies (Fig. 4D). Cells on TCP and collagen were distinctly stratified in two size clusters, with a majority of cells in the larger cluster. In contrast, cells on ECM substrates exhibited a more continuous distribution and were smaller, on average. After 7 days in culture, SVF exhibited greater DNA content on cell-derived ECMs compared to TCP or collagen-coated wells. This effect was maintained over 14 days in culture on MSC- and HDF-derived ECMs, which had greater DNA content compared to all other substrates.

3.3 ECM enhances SVF osteogenic differentiation

SVF can be obtained from several locations including the abdomen, breast, arm, back, and thigh and is commonly subcultured to separate multipotent ASCs from other cell populations. In these studies, ECM promoted osteogenic differentiation of the more heterogeneous SVF derived from multiple donors and donor sites. Importantly, this approach eliminates the need to isolate and expand ASCs in culture prior to use, potentially accelerating the formation of osteogenic grafts. ALP activity, an early and cyclical marker of

osteogenic differentiation, increased in all groups over the first 7 days, with SVF on collagen and MSC-derived ECM demonstrating the lowest levels. After 14 days, SVF on TCP possessed the highest ALP levels. SVF on ECMs exhibited comparable and significantly lower ALP activity compared to TCP, and SVF on collagen had the lowest activity (Fig. 5A). Calcium deposition, a late stage functional output of osteogenic differentiation, increased in all groups over 2 weeks in culture (Fig. 5B). While negligible amounts of calcium were present after 1 day of osteoinduction, confirming the lack of calcium within the secreted ECM, calcium was detectable on cell-derived ECMs after 7 days, with the highest levels evident on MSC-derived ECM. After two weeks in culture, SVF deposited over 8- and 1.3-fold more calcium when cultured on ECM, regardless of source, compared to TCP and collagen-coated controls, respectively. Alizarin red staining confirmed the quantitative values of calcium evidenced by dark red staining throughout the entire well compared to lighter, more diffuse staining when SVF was cultured on TCP or collagen (Fig. 5C). Masson's Trichrome staining revealed differences in matrix content and morphology between all groups (Fig. 5D). SVF on collagen-coated wells exhibited the most intense collagen staining, followed by MSC-derived ECM. Staining on TCP, ASC-, and HDF-derived ECMs was appreciably lighter with patchy regions staining strongly for collagen. However, the magnitude of osteogenic differentiation was comparable for SVF on each cell-secreted ECM, demonstrating the consistency of this material to direct cell fate.

Although SVF from some biological donors produced only minimal levels of calcium on TCP, SVF from all donors produced appreciable calcium in the presence of cell-derived ECMs. In fact, the magnitude of calcium deposition by SVF was significantly greater in all cases (n=4 biological donors) on cell-derived ECMs compared to TCP or collagen (Supplemental Fig. 1). Due to the temporal dependence of ALP expression, heterogeneous nature of cells in SVF expressing ALP, and increased rate of osteogenic differentiation in the presence of cell-derived ECMs,¹¹ the bioactivity of each cell-derived ECM was evaluated using calcium deposition by SVF. In previous studies, we observed increases in MSC osteogenic differentiation using MSC-derived ECMs spanning numerous donors.⁹⁻¹³ In this study, osteogenic differentiation in SVF was consistently increased across ECM produced by several biological donors for MSCs (n=3), ASCs (n=3) and HDFs (n=3) (Fig. 5E), demonstrating the robustness of cell-derived ECM as an instructive biomaterial. While SVF donors were generally healthy, factors such as age, gender, unknown health conditions, and tissue compartment may have contributed to donor-to-donor variation in osteogenic potential.³⁴ Current reports addressing the impact of age, gender, and co-morbidities on the proliferative and osteogenic potential of SVF are contradictory^{35, 36} and warrant continued investigation.

To evaluate the potency of cell-derived ECM, we investigated two doses of protein density for calcium deposition by SVF (Fig. 5F). We selected $15 \mu\text{g cm}^{-2}$ to match the concentration deposited by MSCs during the 10-day ECM deposition period and $7.5 \mu\text{g cm}^{-2}$ as a half-dose to study a significantly lower ECM concentration. At the higher dose, SVF deposited similar quantities of calcium on all ECMs and outperformed SVF on both collagen-coated and TCP controls. At the lower dose, SVF maintained higher calcium deposition on MSC- and ASC-derived ECMs, yet SVF on HDF-derived ECM deposited similar calcium as an equal quantity of collagen. The ability of MSC- and ASC-derived ECMs to maintain

superior osteoinductive capacity over HDF-derived ECM is not surprising due to the greater complexity of proteins represented in MSC- and ASC-derived ECMs. The complex milieu of cell-derived ECMs presents greater opportunities to bind growth factors and retain heterogeneous cell populations *via* activation of diverse integrin pairs when compared to a single ECM molecule such as collagen.^{37, 38}

3.4 ECM promotes the retention of accessory cells to enhance SVF osteogenic differentiation

Specific subpopulations present in SVF and their interactions play a critical role in calcium deposition and vessel formation.³⁹ Furthermore, minimal manipulation of SVF may expedite or obviate FDA approval and reduce translation time to clinical application. Flow cytometry revealed that more than 10% of cells within freshly isolated SVF were CD31+, a classical endothelial cell marker (Fig. 6A). Stromal cells secrete vascular endothelial growth factor that may stimulate proliferation of endothelial cells⁴⁰ and promote neovascularization to preserve viability of engineered tissue *in vivo* and reduce risk of central necrosis. In turn, endothelial cells increase the osteogenic differentiation of osteoprogenitor cells by expression of bone morphogenetic protein-2 (BMP-2), an effect that is abrogated by knockdown of BMP-2 production.^{40, 41} After 14 days of osteoinduction, fewer than 0.1% of cells on TCP were CD31+ (Fig. 6B). However, concomitant with increased osteogenic differentiation, the percentage of CD31+ cells increased on collagen-coated wells and was significantly improved on ECM-coated wells. Similarly, retention of CD34+ cells was increased on collagen- and ECM-coated wells (Fig. 6B), indicating a role for these accessory cells in osteogenic differentiation.

Calcium secretion by SVF was compared to ASCs to assess the contribution of endothelial cells to osteogenic differentiation (Fig. 6C). Regardless of substrate, ASCs deposited significantly less calcium compared to SVF. In fact, when the dose of protein was reduced from 15 $\mu\text{g cm}^{-2}$ to 7.5 $\mu\text{g cm}^{-2}$, ASCs were unable to mineralize their matrix. Calcium deposition by SVF was also ECM dose-dependent, yet SVF on the lower ECM dose deposited more calcium than ASCs on the higher ECM dose. To determine the impact of accessory cells on ASC differentiation, the osteogenic potential of unfractionated SVF was compared to its donor-matched ASC or ASC/endothelial cell (EC) co-culture counterparts. Magnetic-activated cell sorting (MACS) was used to separate donor-matched ASCs and endothelial cells (ECs) for expansion from freshly isolated SVF. After 14 days, all groups exhibited similar DNA content except SVF cultured on MSC-derived ECM, which had significantly higher DNA content compared to all other groups (Fig. 6D). SVF cultured on ASC-derived ECM also exhibited greater DNA content, yet significantly less than SVF on MSC-derived ECM. Consistent trends demonstrating a dip in ALP activity for expanded ASCs compared to SVF and ASC/EC co-culture counterparts were observed across culture substrates (Fig. 6E). However, this trend only reached statistical significance for cells cultured on HDF-derived ECM. As observed with previous donors, calcium deposition by SVF was enhanced on all cell-derived ECMs compared to TCP or collagen, where calcium deposition was minimal, regardless of cell composition (Fig. 6F). ASCs on cell-derived ECMs deposited significantly less calcium compared to their SVF counterpart. While the addition of ECs did not impact calcium deposition on ASC- or HDF-derived ECM, calcium

deposition by the ASC/EC co-culture was restored to the level of SVF on MSC-derived ECM. Interestingly, in both TCP and collagen-coated groups where accessory cell retention was previously demonstrated to be poor, the removal or re-introduction of cells from SVF did not impact calcium deposition. These data confirm the capacity of ECMs to support endothelial cell adhesion and survival but suggest additional accessory cells removed during MACS (*e.g.*, CD34+ cells) and their interactions with the collective cell population may be critical to increase osteogenic differentiation of SVF.

4. CONCLUSION

Decellularized cell-secreted ECMs provide the complex signaling available only by presenting numerous ligands in a biomimetic manner.^{13, 42, 43} However, there is little evidence as to whether there are differences in the instructive potential of ECM secreted by various cell types. Despite differences in ECM composition as a function of cell source, these findings demonstrate the superior capacity of cell-secreted ECM compared to collagen, a single ECM molecule, to serve as an osteoinductive biomaterial for SVF. In fact, this effect was independent of the ECM-depositing cell, implicating the complex niche of signaling cues and ligands present within cell-derived ECM as the driving factor. Moreover, cell-derived ECM preserved accessory cell populations present in SVF, thereby maintaining the inherent vasculogenic potential of a clinically accessible cell source for bone tissue engineering. These studies were performed in monolayer, but the true impact may be achieved in 3-dimensions when complex geometries and material properties (*i.e.* stiffness, porosity, degradation kinetics) can further inform cell behavior and osteogenesis. Others reported the retention of hematopoietic cells in 3D and its value in expanding MSCs for clinical use.^{44, 45} The capacity to form osteogenic grafts through ECM-mediated retention of the heterogeneous SVF population within 3D biomaterials warrants further investigation.

Supplementary Material

Refer to Web version on PubMed Central for supplementary material.

Acknowledgments

This work was supported by grants from the California Institute for Regenerative Medicine (Grant Number RT3-07981), the National Institutes of Health (NIDCR DE025899), and the UC Davis Veterinary Institute for Regenerative Cures to JKL. The content is solely the responsibility of the authors and does not necessarily represent the official views of the National Institutes of Health, CIRM or any other agency of the State of California. The funders had no role in the decision to publish, or preparation of the manuscript. JNH received support from the National Defense Science and Engineering Graduate Fellowship (32 CFR 168a), Schwall Fellowship in Medical Research and Achievement Rewards for College Scientists (ARCS) Foundation. The authors acknowledge Andrea Kulinich for assistance with cell culture.

References

1. Hynes RO. *Science*. 2009; 326:1216–1219. [PubMed: 19965464]
2. Reyes CD, Petrie TA, Garcia AJ. *J Cell Physiol*. 2008; 217:450–458. [PubMed: 18613064]
3. Barker TH. *Biomaterials*. 2011; 32:4211–4214. [PubMed: 21515169]
4. Cheng CW, Solorio LD, Alsberg E. *Biotechnol Adv*. 2014; 32:462–484. [PubMed: 24417915]
5. Marinkovic M, Block TJ, Rakian R, Li Q, Wang E, Reilly MA, Dean DD, Chen XD. *Matrix Biol*. 2016; 52–54:426–441.

6. Subbiah R, Hwang MP, Du P, Suhaeri M, Hwang JH, Hong JH, Park K. *Macromol Biosci.* 2016; 16:1723–1734. [PubMed: 27557868]
7. Tour G, Wendel M, Tcacencu I. *J Biomed Mater Res A.* 2013; 101:2826–2837. [PubMed: 23471711]
8. Lai Y, Sun Y, Skinner CM, Son EL, Lu Z, Tuan RS, Jilka RL, Ling J, Chen XD. *Stem Cells Dev.* 2010; 19:1095–1107. [PubMed: 19737070]
9. Decaris ML, Binder BY, Soicher MA, Bhat A, Leach JK. *Tissue Eng Part A.* 2012; 18:2148–2157. [PubMed: 22651377]
10. Decaris ML, Leach JK. *Ann Biomed Eng.* 2011; 39:1174–1185. [PubMed: 21120695]
11. Decaris ML, Mojadedi A, Bhat A, Leach JK. *Acta Biomater.* 2012; 8:744–752. [PubMed: 22079209]
12. Harvestine JN, Vollmer NL, Ho SS, Zikry CA, Lee MA, Leach JK. *Biomacromolecules.* 2016; 17:3524–3531. [PubMed: 27744699]
13. Hoch AI, Mittal V, Mitra D, Vollmer N, Zikry CA, Leach JK. *Biomaterials.* 2016; 74:178–187. [PubMed: 26457835]
14. Ragelle H, Naba A, Larson BL, Zhou F, Prijic M, Whittaker CA, Del Rosario A, Langer R, Hynes RO, Anderson DG. *Biomaterials.* 2017; 128:147–159. [PubMed: 28327460]
15. Bourin P, Bunnell BA, Casteilla L, Dominici M, Katz AJ, March KL, Redl H, Rubin JP, Yoshimura K, Gimble JM. *Cytotherapy.* 2013; 15:641–648. [PubMed: 23570660]
16. Mitchell JB, McIntosh K, Zvonic S, Garrett S, Floyd ZE, Kloster A, Di Halvorsen Y, Storms RW, Goh B, Kilroy G, Wu X, Gimble JM. *Stem Cells.* 2006; 24:376–385. [PubMed: 16322640]
17. Strioga M, Viswanathan S, Darinskas A, Slaby O, Michalek J. *Stem Cells Dev.* 2012; 21:2724–2752. [PubMed: 22468918]
18. Barbosa I, Garcia S, Barbier-Chassefiere V, Caruelle JP, Martelly I, Papy-Garcia D. *Glycobiology.* 2003; 13:647–653. [PubMed: 12773478]
19. Mitra D, Fatakawala H, Nguyen-Truong M, Creecy A, Nyman J, Marcu L, Leach JK. *ACS Biomater Sci Eng.* 2017; 3:1944–1954. [PubMed: 28944287]
20. Charvet HJ, Orbay H, Harrison L, Devi K, Sahar DE. *Ann Plast Surg.* 2016; 76(Suppl 3):S241–245. [PubMed: 27070671]
21. Brown WE, Hu JC, Athanasiou KA. *Tissue Eng Part C Methods.* 2016; 22:895–903. [PubMed: 27553086]
22. Schmittgen TD, Livak KJ. *Nat Protoc.* 2008; 3:1101–1108. [PubMed: 18546601]
23. Hoch AI, Binder BY, Genetos DC, Leach JK. *PloS one.* 2012; 7:e35579. [PubMed: 22536411]
24. Swinehart IT, Badylak SF. *Dev Dyn.* 2016; 245:351–360. [PubMed: 26699796]
25. Xue JX, Gong YY, Zhou GD, Liu W, Cao Y, Zhang WJ. *Biomaterials.* 2012; 33:5832–5840. [PubMed: 22608213]
26. Stern MM, Myers RL, Hammam N, Stern KA, Eberli D, Kritchevsky SB, Soker S, Van Dyke M. *Biomaterials.* 2009; 30:2393–2399. [PubMed: 19168212]
27. Adam Young D, Bajaj V, Christman KL. *J Biomed Mater Res A.* 2014; 102:1641–1651. [PubMed: 24510423]
28. Seif-Naraghi SB, Singelyn JM, Salvatore MA, Osborn KG, Wang JJ, Sampat U, Kwan OL, Strachan GM, Wong J, Schup-Magoffin PJ, Braden RL, Bartels K, DeQuach JA, Preul M, Kinsey AM, DeMaria AN, Dib N, Christman KL. *Sci Transl Med.* 2013; 5:173ra125.
29. Zhang Y, He Y, Bharadwaj S, Hammam N, Carnagey K, Myers R, Atala A, Van Dyke M. *Biomaterials.* 2009; 30:4021–4028. [PubMed: 19410290]
30. Luo B, Yuan S, Foo SE, Wong MT, Lim TC, Tan NS, Choong C. *Adv Healthc Mater.* 2015; 4:613–620. [PubMed: 25424903]
31. Xing Q, Yates K, Tahtinen M, Shearier E, Qian Z, Zhao F. *Tissue Eng Part C Methods.* 2015; 21:77–87. [PubMed: 24866751]
32. Stephansson SN, Byers BA, Garcia AJ. *Biomaterials.* 2002; 23:2527–2534. [PubMed: 12033600]
33. Murphy KC, Hoch AI, Harvestine JN, Zhou D, Leach JK. *Stem Cells Transl Med.* 2016; 5:1229–1237. [PubMed: 27365484]

34. Dufrane D. *Cell Transplant.* 2017; 26:1496–1504. [PubMed: 29113460]
35. Choudhery MS, Badowski M, Muise A, Pierce J, Harris DT. *J Transl Med.* 2014; 12:8. [PubMed: 24397850]
36. Chen HT, Lee MJ, Chen CH, Chuang SC, Chang LF, Ho ML, Hung SH, Fu YC, Wang YH, Wang HI, Wang GJ, Kang L, Chang JK. *J Cell Mol Med.* 2012; 16:582–593. [PubMed: 21545685]
37. Hudalla GA, Murphy WL. *Adv Funct Mater.* 2011; 21:1754–1768. [PubMed: 21921999]
38. Seif-Naraghi SB, Horn D, Schup-Magoffin PJ, Christman KL. *Acta Biomater.* 2012; 8:3695–3703. [PubMed: 22750737]
39. Guven S, Mehrkens A, Saxer F, Schaefer DJ, Martinetti R, Martin I, Scherberich A. *Biomaterials.* 2011; 32:5801–5809. [PubMed: 21605897]
40. Murphy KC, Stilhano RS, Mitra D, Zhou D, Batarni S, Silva EA, Leach JK. *FASEB J.* 2016; 30:477–486. [PubMed: 26443826]
41. Kaigler D, Krebsbach PH, West ER, Horger K, Huang YC, Mooney DJ. *FASEB J.* 2005; 19:665–667. [PubMed: 15677693]
42. Chen XD, Dusevich V, Feng JQ, Manolagas SC, Jilka RL. *J Bone Miner Res.* 2007; 22:1943–1956. [PubMed: 17680726]
43. Prewitz MC, Seib FP, von Bonin M, Friedrichs J, Stissel A, Niehage C, Muller K, Anastassiadis K, Waskow C, Hoflack B, Bornhauser M, Werner C. *Nat Methods.* 2013; 10:788–794. [PubMed: 23793238]
44. Braccini A, Wendt D, Jaquiery C, Jakob M, Heberer M, Kenins L, Wodnar-Filipowicz A, Quarto R, Martin I. *Stem Cells.* 2005; 23:1066–1072. [PubMed: 16002780]
45. Chen X, Xu H, Wan C, McCaigue M, Li G. *Stem Cells.* 2006; 24:2052–2059. [PubMed: 16728560]

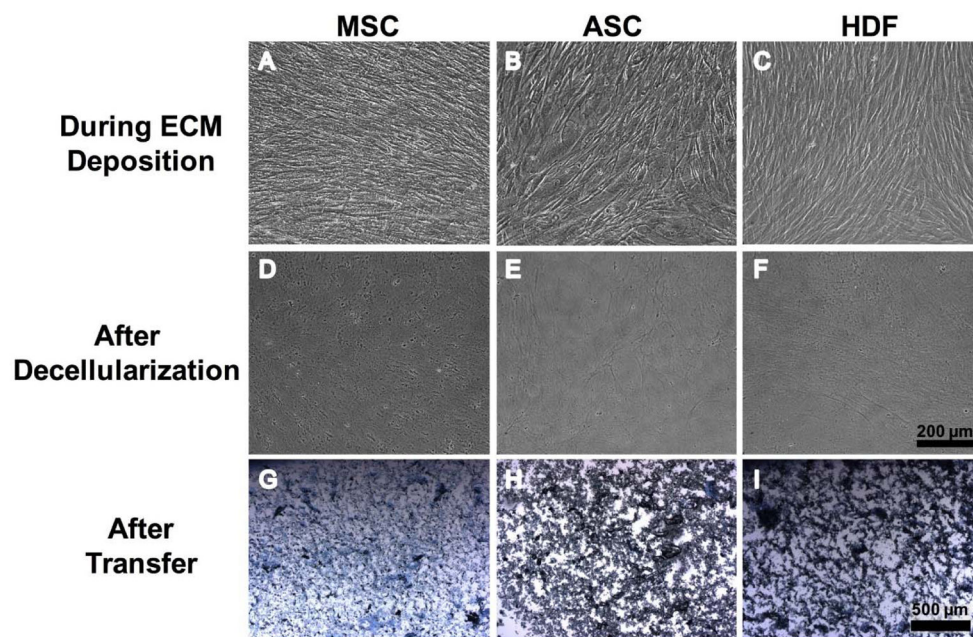


Figure 1. Morphology of MSCs, ASCs, and HDFs in culture and their resulting ECMs (A–C) Brightfield images of cell monolayer on day 10 of ECM deposition and (D–F) decellularized ECM visible on culture surface after cell removal. Scale bar represents 200 µm (10x magnification). (G–I) Equal quantities of ECM stained with Coomassie Brilliant Blue after transfer to the surface of new well plates. Scale bar represents 500 µm (4x magnification).

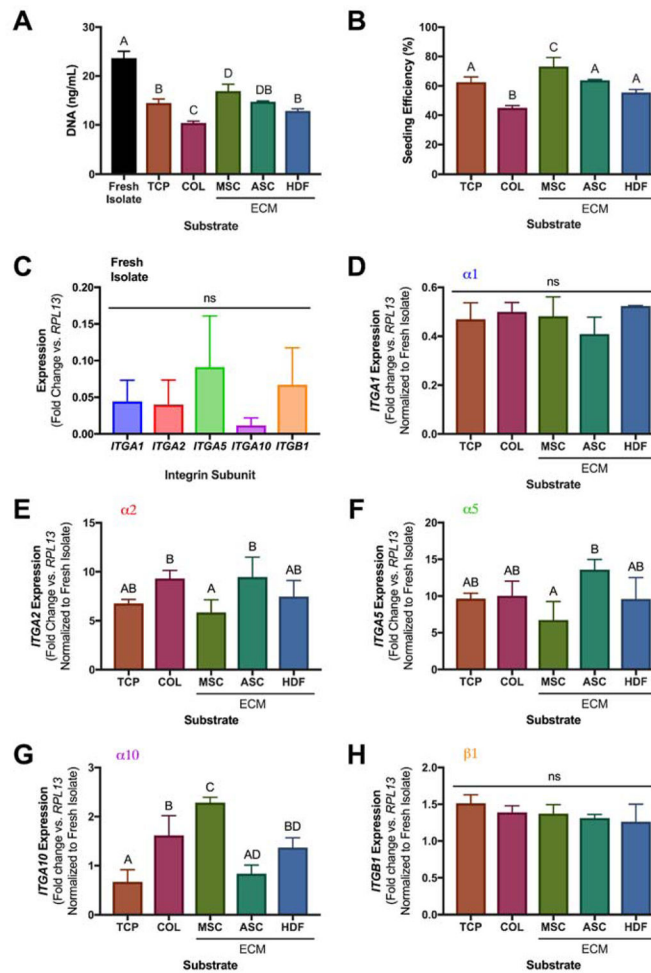


Figure 3. ECM-mediated adhesion of freshly isolated SVF

(A) DNA content of viable cells upon isolation or 7 hours of culture on various substrates (n=4). (B) Seeding efficiency of SVF (n=4). (C) Relative gene expression of integrins involved in adhesion to substrates within freshly isolated SVF (n=4). (D–H) Relative gene expression of integrin subunits after 7 hours in culture (n=4). For (A–H), groups with no significance are linked by the same letters, while groups with significance do not share a letter. Lack of significance between groups is denoted by “ns”.

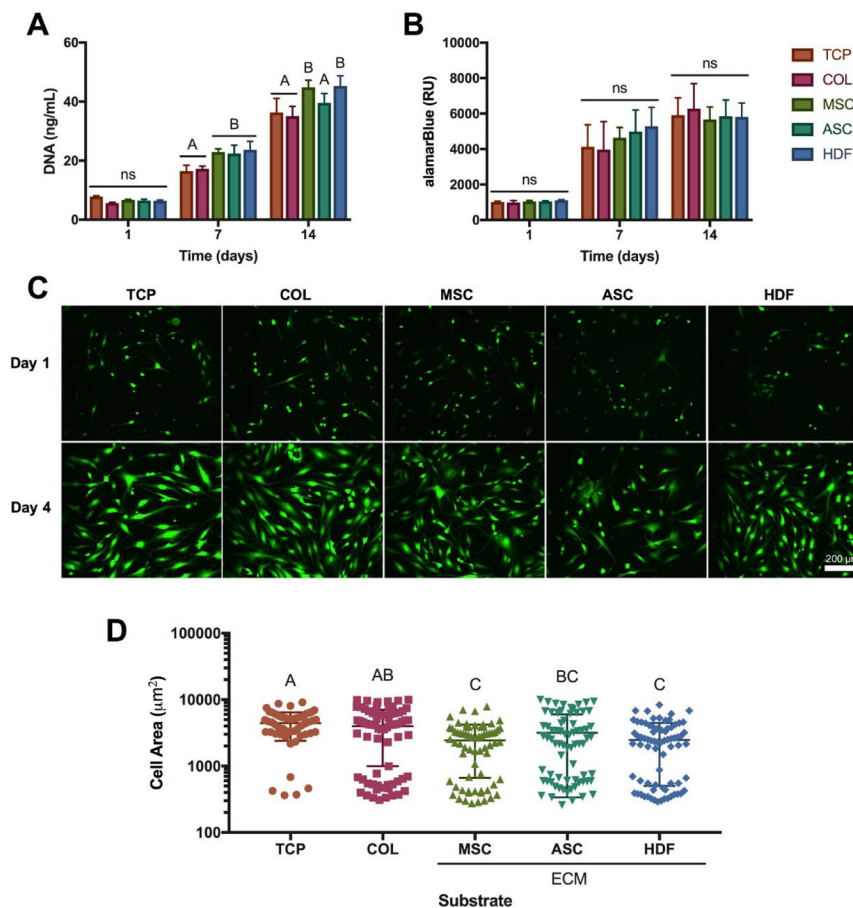


Figure 4. SVF proliferation is supported by all substrates

(A) DNA content over 14 days in culture (n=4). (B) Metabolic activity measured by alamarBlue assay (n=4). (C) Representative images of cells stained with calcein AM at 1 (top row) and 4 days (bottom row) in culture. Images are SVF on TCP, collagen, MSC-, ASC-, or HDF-derived ECM (left to right). Scale bar represents 200 μm (20x magnification). (D) Quantification of cell area (n=16–20 cells per image quantified from n=3 images). For (A, B, D), groups with no significance are linked by the same letters, while groups with significance do not share a letter. Lack of significance between groups is denoted by “ns”.

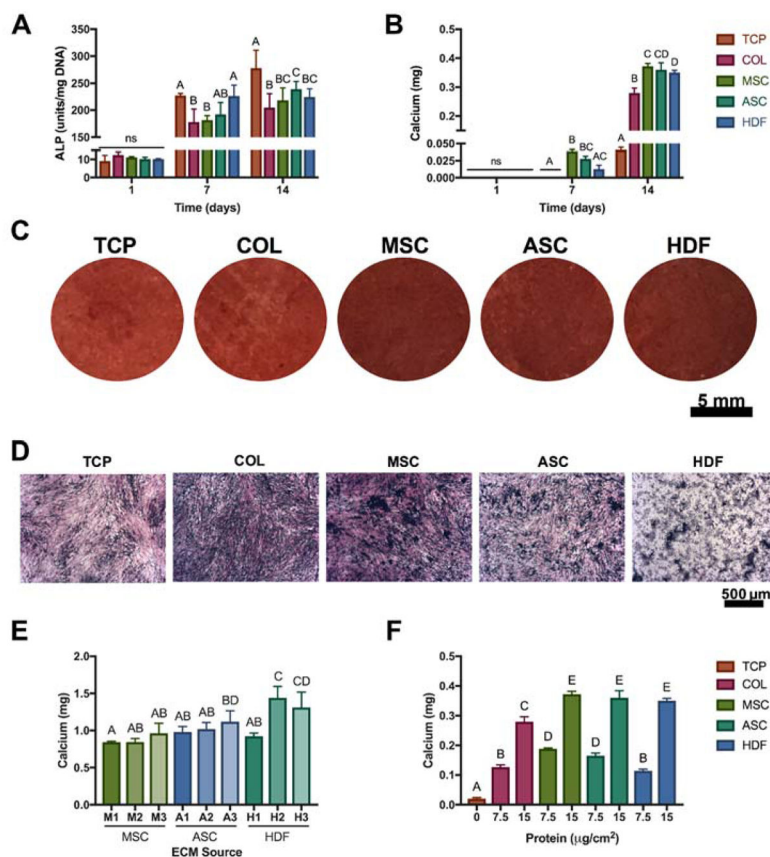


Figure 5. ECM enhances SVF osteogenic differentiation in osteoinductive media

(A) Alkaline phosphatase (ALP) activity of SVF (n=4). (B) Total calcium deposition (n=6). Representative (C) Alizarin red stain for mineralized matrix deposition (Scale bar represents 5 mm) and (D) Masson's Trichrome (Scale bar represents 500 μm) after 14 days in culture. (E) Total calcium deposition after 14 days in culture by 1 biological SVF donor on ECM produced by several biological donors for MSCs (n=3), ASCs (n=3) and HDFs (n=3). (F) Total calcium deposition after 14 days in culture on TCP or low (7.5 $\mu\text{g cm}^{-2}$) and high (15 $\mu\text{g cm}^{-2}$) doses of collagen and ECM. For (A–B, E–F), groups with no significance are linked by the same letters, while groups with significance do not share a letter. Lack of significance between groups is denoted by “ns”.

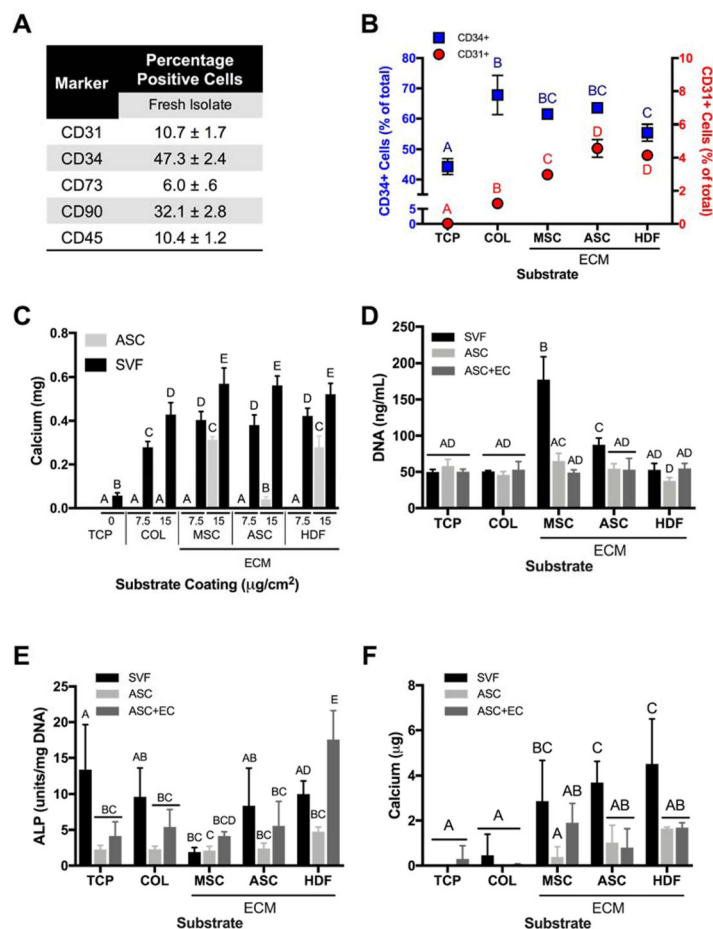


Figure 6. Retention of CD31+ cells on ECM potentiates SVF osteogenic differentiation
(A) Quantification of cell markers present in freshly isolated SVF determined using flow cytometry (n=3). **(B)** Percentage of CD34+ (blue data) and CD31+ (red data) cells remaining after 14 days in osteogenic media. Letters denote differences within a single CD marker. Groups with no significance are linked by a shared letter and groups with significance do not share a letter. (n=3). **(C)** Total calcium deposition by ASCs or SVF after 14 days in culture on TCP or low (7.5 $\mu\text{g cm}^{-2}$) and high (15 $\mu\text{g cm}^{-2}$) doses of collagen and ECM (n=4). **(D–F)** Osteogenic potential of donor-matched samples by quantification of **(D)** total DNA content, **(E)** ALP activity, and **(F)** calcium deposition by SVF, expanded ASCs, or co-culture of expanded ASCs and endothelial cells (ECs) after 14 days in osteogenic media (n=3–4). For **(B–F)**, groups with no significance are linked by the same letters, while groups with significance do not share a letter. Lack of significance between groups is denoted by “ns”.

Non-collagenous osteogenic, pro-angiogenic, and immunomodulatory proteins identified from ECM mass spectrometry analysis. The highest, medium, and lowest relative percentages between MSC-, ASC-, and HDF-derived ECMs are highlighted in red, yellow, and green, respectively.

Table 1

Protein	Accession	Biologic Function	Relative Percentage (%)		
			MSC	ASC	HDF
Fibronectin	P02751	Promotes cell adhesion and motility and is essential for osteoblast mineralization	2.700%	1.800%	0.710%
Periostin	Q15063	Enhances BMP1 incorporation in the fibronectin matrix, and subsequent proteolytic activation of lysyl oxidase (LOX)	0.660%	0.540%	0.130%
Lysyl-Oxidase Homolog 2	Q9Y4K0	Collagen crosslinking enzyme resulting in more mature, mechanically robust tissues	0.220%	0.240%	0.000%
Perlecan	P98160	Vascular extracellular matrix protein that stimulates endothelial growth and regeneration	0.370%	0.210%	0.020%
Emilin-1	Q9Y6C2	Guides lymphatic endothelial cells for lymphatic vessel formation	0.890%	0.510%	0.390%
Annexin-1	P04083	Promotes resolution of inflammation and wound healing	0.304%	0.153%	0.182%
Galectin-1	P09382	Supports immunomodulation by apoptosis of activated immune cells	1.422%	2.778%	0.948%
Glycerinaldehyde-3-phosphate dehydrogenase	P04406	Inhibits inflammatory response	1.251%	0.331%	0.790%
Filamin-A	P21333	Important in cell-cell contacts and adherens junctions during the development of blood vessels, heart and brain organs	0.641%	0.000%	0.160%
Ras-related protein Rap-1b	P61224	Establishment and maintenance of endothelial cell polarity and vascular lumen	0.226%	0.000%	0.226%